CHAPTER TWO HUNDRED TWO

NUMERICAL MODELING OF SHORELINE EVOLUTION AROUND THE RIVER MOUTH

MING-CHUNG LIN* and JYH-CHERNG WANG**

1.0 INTRODUCTION

The river sediments transport into coastal water together with wave-induced longshore sediment transport make shoreline evolution much complicated. Fig.1 shows typical feature of shoreline shape around a river mouth. Recently there are some investigators treated this problem(Grijm, 1964, Bakker & Edelmen,1964; Komar,1973; Tsuchiya & Yasuda,1978),and had developed some mathematical or numerical models. This paper proposes a numerical model for predicting long-term shoreline evolution around a river mouth by incorporation certain river parameters into the Willis beach evolution model (1978). The proposed model is at first applied to four ideal cases to investigate its general characteristics and adaptability, and reasonable results are found. In our results the accretion on updrift side is faster than downdrift side under the oblique incident wave condition and the width of the river mouth increase steadily. These results are different from other approachs that the shoreline shape is always nearly symmetrical with respect to the centerline of the river mouth. Finally, as an field case application of the model, a numerical simulation of shoneline changes around the Cho-shui River mouth is performed and compared with field data.

2.0 FORMULATION OF THE MODEL

2.1 Assumptions

In order to make the problem tractable, we make some basic assumptions:

(1) A year is divided into some periods, and in each period the wave characteristics such as height H_o, period T_o and length L_o are const..
(2) Wave will break at the place where water depth is equal to 1.25 H_o.
(3) The energy of breaking wave will not exceed five times of offshore wave. The excuding energy, if any, will be distributed to the elements of each side.
(4) The upper swash limit of waves equal to mean high water level plus one breaking wave height; the critical water depth of sediment movement is twice breaking waves height below the mean low water level.
(5) The sand transport by wind, tidal current and the artificial effect will leave out of consideration.
(6) The wave-induced alongshore discharge and the river-induced alongshore discharge can be a linear accumulation.

*Professor, Dept. of Naval Architecture, National Taiwan University, Taipei, Taiwan, 107, R.O.C.

**Senior Coastal Enginner, China Engineering Consultants, Inc., Taipei, Taiwan, R.O.C.

(7) A year is divided into some periods, and the discharge, and the sediment concentration of the river in a period are constant.

2.2 Shoreline Evolution Equations

In the proposed model we consider two regions. One is coastal region away from river mouth, in which no river discharge and sediment directly flow into the elements. The other is river mouth region.

(1) Coastal region

As Willis (1978), the sand transport zone is schematized as a triangle prism bounded by the instantaneous mean water level, the flat sloping bed and a depth equal to twice the average breaking wave height (Fig. 2). The alongshore discharge and sediment flow into the element equal to $Q_x\Delta t$ and $C_nQ_x\Delta t$ repectively. The amount of flowing out are

$$\left[Q_x + \frac{\partial Q_x}{\partial x} \Delta x \right] \Delta t + Q_{n\omega}\Delta t$$

$$\left[C_n + \frac{\partial C_n}{\partial x} \Delta x \right] \left[Q_x + \frac{\partial Q_x}{\partial x} \Delta x \right] \Delta t + C_{n\omega} Q_n \Delta t$$

According to the continuity of discharge we will get

$$Q_{n\omega} = - \frac{\partial Q_x}{\partial x} \Delta x \qquad (1)$$

by applying the continuity to sediment transport within the element, it yields

$$\left[C_n + \frac{\partial C_n}{\partial x} \Delta x \right] \left[Q_x + \frac{\partial Q_x}{\partial x} \Delta x \right] \Delta t + C_{n\omega} Q_{n\omega}\Delta t$$

$$= C_n Q_x \Delta t - (D2\text{-}F)\Delta Y\Delta x \qquad (2)$$

here the sediment transport is expressed as the product of flow discharge and sediment concentration.

Subsituting Eq.(1) into Eq.(2) then yields

$$(D2\text{-}F) \frac{\Delta Y}{\Delta t} + (C_n - C_{n\omega}) \frac{\partial Q_x}{\partial x} + Q_x \frac{\partial C_n}{\partial x} + \frac{\partial C_n}{\partial x} \frac{\partial Q_x}{\partial x} \Delta x = 0 \qquad (3)$$

where

(D2-F) = vertical distance from the upper swash limit of waves to the critical water depth of sediment movement

Q_x = alongshore discharge which is equal to QL + QW_x ; QL

denotes the river-induced alongshore discharge, QW_x denotes the wave-induced alongshore discharge.

Q_n = onshore-offshore discharge.

C_n = alongshore sediment concentration.

$C_{n\omega}$ = onshore-offshore sediment concentration

The shoreline change Δy of coastal region can be calculated by Eq. (3). The form of this equation (3) is the same as that of Willis. But we must point out that herein Q_x is different from that of the Willis equation.

(2) River mouth region

In this region river discharge QR_n and river sediment $C_{nR}\ QR_n$ are taken into account in the elements. By the continuity equation of discharge we can get

$$Q_{n\omega} = -\frac{\partial Q_x}{\partial x}\Delta x + QR_n \tag{4}$$

By the sediment continuity equation we get

$$Q_x C_n \Delta t + QR_n C_{nR}\Delta t - \left[Q_x + \frac{\partial Q_x}{\partial x}\Delta x\right]\left[C_n + \frac{\partial C_n}{\partial x}\Delta x\right]\Delta t$$

$$- C_{n\omega}\, Q_{n\omega}\, \Delta t = (D2\text{-}F)\Delta Y \Delta x \tag{5}$$

From Eq.(4) and Eq.(5) it yields readily

$$(D2\text{-}F)\frac{\Delta Y}{\Delta x} + (C_n - C_{n\omega})\frac{\partial Q_x}{\partial x} + Q_x \frac{\partial C_n}{\partial x} + \frac{\partial C_n}{\partial x}\frac{\partial Q_x}{\partial x}\Delta x$$

$$+ (C_{n\omega} - C_{nR})\frac{QR_n}{\Delta x} = 0 \tag{6}$$

The shoreline change Δy of river mouth region then can be computed by Eq.(7). For solving Eq.(3) and Eq.(6) the evaluations of QL_n, QW_x, C_n and $C_{n\omega}$ are needed in advance.

2.3 The River-induced Alongshore Discharge

We here model the flow at river mouth by a turbulent plane jet flow. Fig. 3 shows the elements schemed and the flow distribution. For the center element 1, the river discharge flowing in is QR_1 and the jet discharge flowing out is QO_1. By applying continuity equation, we get alongshore current dischange induced by river at element 1

$$QL_1 = KR\,\frac{QR_1 - QO_1}{2} \tag{7}$$

where KR is a modification factor. When performing numerical calculation afterward, we take it to be 1.0. Similarly, the river-induced alongshore current discharge in the element n can be expressed as

$$QL_n = KR\ (QR_n - QO_n) + QL_{n-1} \tag{8}$$

If $|x|$ is larger than b_o, the QR_n is equal to zero. If the $|x|$ is larger than the boundary of the jet velocity distribution, we assume the alongshore discharge will be decreased in the manner of the form:

$$QL_{n+m} = QL_n / (1+m)^2 \tag{9}$$

Where QO_n can be obtained by integrating the velocity distribution of a turbulent plane jet flow. In the present study, the velocity distribution in turbulent plane jet interacting with obliquely incident wave developed by Hwung & Chen (1981) is used. Fig. 4 shows the coordinate system they used. Hwung and Chen assumed that the velocity distribution be a Gaussian distribution for a wave period average.

$$\frac{\bar{u}\ (x,y)}{[\bar{u}\ (o,y)]_{max}} = \exp\left(-\frac{x^2}{2C_1 y^2}\right) \tag{10}$$

in which C_1 is a velocity distribution coefficient. By momentum conservation concept, it reads

$$[u(o,y)]_{max} = \left\{\frac{2\ b_o}{1+0.5\alpha^2(y,\theta)\sqrt{\pi}\ C_1 y}\right\}^{0.5} u_o \tag{11}$$

where

$$\alpha(y,\theta) = \sqrt{\frac{2\ \frac{\bar{u}_\omega^2}{u_o^2}\ \sqrt{\pi}\ C_1\ \frac{y}{b_o}\ \cos^2\theta}{2 - \frac{\bar{u}_\omega^2}{u_o^2}\ \sqrt{\pi}\ C_1 \frac{y}{b_o}\ \cos^2\theta}} \tag{12}$$

$$\bar{u}_\omega^2 = \frac{\pi H^2}{2T^2}\ \coth^2\left(\frac{2\pi h}{L}\right) \tag{13}$$

Where h denotes water depth.

The width of velocity distribution is expressed as

$$\frac{b(y,\theta)}{b_o} = \sqrt{\frac{\pi}{2}}\ C_1\ \frac{y}{b_o} + \frac{\varepsilon(y,\theta)}{b_o \alpha(y,\theta)} \tag{14}$$

Where

$$\varepsilon(y,\theta) = \frac{\pi H}{L}\ \coth\left(\frac{2\pi d}{L}\right)\ \sqrt{\pi}\ C_1 y\ \cos^2\theta \tag{15}$$

Here H, L, d denote the wave height, wave length, and water depth respectively. From Eq.(11) – Eq.(16) $\bar{u}(x,y)$ can be calculated and then QO_n can be obtained.

In the present study, when numerical calculation is performed, wave refraction is calculated by the Brampton model (1977), wave-induced longshore current and discharge by the Willis (1978a) work and sediment concentration by the Willis (1978b) formula.

3.0 NUMERICAL FORMULATION

3.1 Difference Form of Shoreline Evolution Equation

Fig. 5 shows the differential element layout, in which y_n is the distance from baseline to the middle of the upper swash limit and the critical water depth of sediment movement. We set

$$y_{n-\frac{1}{2}} = \frac{1}{2}\left(y_{n-1} + y_n \right) \tag{16}$$

And the angle between shoreline and baseline A_s at gride n is

$$A_s(n,t) = \tan^{-1}\left[\frac{y(n+\frac{1}{2},t) - y(n-\frac{1}{2},t)}{\Delta x} \right] \tag{17}$$

The angle between shoreline and wave crest line A_{br} then can be got by A_s. Now let

$$DQ = Q_x(n+1,t) - Q_x(n,t)$$

$$DC = C_n(n+1,t) - C_n(n,t)$$

$$Q_{ave} = \frac{1}{2}\left[Q_x(n+1,t) + Q_x(n,t) \right]$$

$$QR_{ave} = \frac{1}{2}\left[QR(n+1,t) + QR(n,t) \right]$$

$$DNC = \frac{1}{2}\left[C_n(n+1,t) + C_n(n,t) - C_{n\omega}(n+1,t) - C_{n\omega}(n,t) \right]$$

$$DNR = \frac{1}{2}\left[C_{n\omega}(n+1,t) + C_{n\omega}(n,t) - C_{nR}(n+1,t) - C_{nR}(n,t) \right]$$

then, from Eq.(3), difference equation for coastal region is

$$DY = \frac{\Delta t}{(D2-F)\Delta x}\left[DQ \times DNC + Q_{ave} \times DC + DC \times DQ \right] \tag{18}$$

and the difference form of Eq.(6) in river mouth region is

$$DY = \frac{\Delta t}{(D2-F)\Delta x}\left[DQ \times DNC + Q_{ave} \times DC + DC \times DQ + DNR \times QR_{ave} \right] \tag{19}$$

3.2 Input Data

The proposed model needs the following input data

(1) The height, direction, period and length of incident wave in each calculated period, and the duration of each period in a year.

(2) The location, discharge, sediment concentration and width of river in each period, and the duration of each period in a year.

(3) The kinematic viscosity and density of sea water.

(4) Density, porosity, D_{50} of sand, and the relative roughness.

(5) Mean high water level and mean low water level.

(6) The initial water depth chart.

(7) The other special data, such as no-erosible region or coastal structure.

4.0 NUMERICAL RESULTS OF FOUR IDEAL CASES

4.1 Input Data of Four Ideal Cases

For investigating the general characteristics and adaptability of the proposed model, we run four ideal cases. The same part of input data are as follows:

(1) beach slope 0.01
(2) Kinematic viscosity of fluid 1.3×10^{-6} m^2/S
(3) Density of sea water 1020 kg/m^3
(4) Density of sand 2650 kg/m^3
(5) Porosity of sand 0.35
(6) Central grain diameter 0.0002 m.
(7) Width of river mouth 1.2 Km
(8) Relative roughness of sand 0.0007m
(9) River flow velocity at mouth 0.6 m/S
(10) Incident wave height 2 m

Table 1 shows the other input data for each case.

Table 1 Input data for four ideal cases

	The depth of river (m)	River Discharge (cms)	River sediment concentration	Wave incident angle (°)
Case A	1.5	1080	0.0004	45
B	1.0	720	0.0006	45
C	1.0	720	0.0004	45
0	1.0	720	0.0004	30

4.2 The Features of the Present Model

The numerical results are shown in Fig.6. From these results, some important features can be described as follows.

(1) In all cases the accretion on updrift side is faster than downdrift side under the assumed oblique incident wave condition.

(2) In all cases the width of the river mouth increase steadily and the center lines are alway refracted to the direction of nearshore current.

(3) Fig. 6a shows the results of case A and B, which indicate that when the total sediment transport of river is constant, an increase in river discharge will decrease the accretion of downdrift side.

(4) Fig. 6b shows the results of case B and C, which indicate that when river discharge is equal, the accretion of each drift side is in proportion to sediment concentration.

(5) Fig. 6c shows the results of case A and C, which indicate that if sediment concentration is equal, the accretion of updrift side increases with river discharge increase, but in downdrift side is just opposite.

(6) Fig. 6d shows the results of case C and D, which indicate that if all input data of the river is the same, the accretion of updrift side increases with wave-induced nearshore current velocity increase, but in downdrift side is just opposite.

5.0 FIELD CASE APPLICATION OF THE MODEL

5.1 Introduction

Cho-Shui River, located in the mid-west Taiwan, is the biggest one in Taiwan. The annual total discharge is about 4.65×10^9 m^3/year. The total sediment load is about 4×10^7 m^3/year, among which 1×10^7 m^3/year of sediment load being deposited on the river bed and the left 3×10^7 m^3/year sediment load flowing into the coastal water and settled down the river mouth. Due to the river flow and incident wave, the shoreline evolution is severe and complicated. Fig. 7 shows the change of the shoreline around the Cho-Shui river between 1903 and 1972. Before 1911 the Cho-Shui river use the channel of the old Cho-Shui river, but after a work of channel regulation done in 1911, the mouth of the Cho-Shui river was changed to the present location. The change get a severe erosion of the shoreline around the Old Cho-Shui river mouth and a great accretion around the Present Cho-Shui river mouth.

5.2 Description of Input Data

(1) The variation of the discharge and the sediment concentration of the Cho-Shui river is very large. Table 2 shows the various data of discharge in a year at the Silo station. It is quite difficult to choose the amount of discharge in each period

Table 2. Discharge of Cho-Shui River (Unit: Cms)

Item \ Month	1	2	3	4	5	6	7	8	9	10	11	12
Monthly average	6.91	6.61	17.39	30.05	122.30	412.43	170.77	317.36	194.70	91.26	30.86	18.77
Max. monthly average	31.28	51.40	108.07	195.98	364.22	1,058.03	569.90	878.68	480.32	269.26	226.10	70.38
Min. monthly average	0.33	0.31	0.46	0.49	4.19	24.96	8.70	22.01	14.16	5.43	3.24	5.31

Average discharge	Max. annual average	Min. annual average	Max. day average	Min. day average
122.95	208.34	36.23	6,610.00	0.09

Table 3. Input data combination

Time step \ Item	Duration (month)	Wave direction	Wave height (m)	Waver period (s)	Discharge (cms)	Sediment concentration	Sediment load (m^3/month)
1	8.3	NE	1.63	5.50	2,100	0.0006	3.26×10^6
2	3.7	SW	0.70	5.00	500	0.0006	7.78×10^5

for use. It is also not easy for selecting correctly the sediment concentration by its large variation from 40 ppm to 3500 ppm. For deciding reasonablly the discharge and the sediment concentration of the river, we had made a several tests for several combinations. Considering the fact that the proposed model is more suitable for large discharge, we finally suggest taking a discharge larger then the real discharge in each period. This discharge combining with the sediment concentration, which is little than the real average concentration, make sure the total sediment load equal to the real total load. The combination we take is shown in table 3.

(2) According to the report of Taichung Harbour Bureau (1973), we decide the incident wave height and period in monsoon and summer season as shown in table 3.

(3) For the initial water depth chart we used the sea chart No.234 of Japanese Navy Waterway survey department in 1903. Fig.8 shows the water depth in the scope we decided. This scope includes the old Cho-Shui River in order to understand the effect of the Cho-Shui river channel regulation in 1911.

(4) The other input data we used just as follow:

kinematic viscosity of sea water	1.3×10^{-6} m^2/s
density of sea water	1020 kg/m^3
density of sand	2650 kg/m^3
widtn of river mouth	2.1 km
central grain diameter	0.0002 m
sand relative roughness	0.0007 m
porosity of sand	0.35

5.3 The Result of The Numerical Simulation

Fig. 9 shows the simulated result. The centerline of the Cho-Shui river is at the grid 27.5 in x-axis. The result is not good enough because we had not considered the artificial effect just like oyster and other water fowls growth. In the following some discussions about the result is described for three regions.

(1) The region 1 is from grid 40 to grid 55, being just at the south side of the old Cho-Shui river mouth. Either the sea chart or our simulation result show this region had a quickly accretion from 1903 to 1972. But the accretion velocity of the sea cbart is large than the simulation one. For understanding the reason we investigated the shoreline of this region and found that there were many oyster growth fields there. These oyster grouth fields had made a large deposition of the longshore sediment load beyond the nature quantity. It seems that the existence of this artificial oyster fields make the deviation of numerical result.

(2) The region 2 from gird 20 to gride 40 is just at the Cho-Shui river

mouth. Either the field or numerical result showed this region also had a quickly accretion from 1903 to 1972, and a delta had been grown. The location of the delta in our simulation result is at the north side of the field one, but the accretion velocity was almost equal, and the area of accretion in region 1 and region 2 in simulation is almost equal to that of the field result. Consequently this unagrement between numerical and field result might be due to the over deposition in region 1.

(3) In the region 3 from grid 10 to gride 20, which is at the south side of the Cho-Shui river mouth, there are no artificial oyster grouth and other coastal structures. The simulation result agree the field data very well.

From the fact metioned above, if there are no artificial effects, the present model would be able to give a reasonable agreement.

6.0 CONCLUSIONS

According to the results descriped above, we get some conclusions:

(1) The proposed model assumes that the river flow in the coast around the river mouth is a turbulent plane jet. So the model is more suitable for the rivers with large discharge and velocity.

(2) The other approachs either mathematical solutions or numerical simulations always lead to unreasonable results that the shoreline shape is nearly symmetrical with respect to the centerline of river mouth even if oblique wave approaches, and that under constant river sediment supply the shape of shoreline at the river mouth maintains no change even though the river discharge or sediment concentration is changed. The proposed model, in contrast, can give more reasonable results with more general conditions.

(3) The proposed model can be used readily for field cases to predict the shoreline evolution around the river mouth.

REFERENCES

Acker, P. and W. R. White, 1973: Sediment Transport, New Approach and Analysis, Proc. ASCE, Vol.99, No. HY-11, 2041-2060.

Brampton, A. H., 1977: A Computer Method for Wave Refraction, Hydraulic Research Station, Rept. No. IT-172.

Bakker, W. T. and T. Edelman, 1964: The Coastline of River-Delats, Proc. of the 9th Conf. on Coastal Eng., ASCE, 199-218.

Grijm, W., 1964: Theoretical Formes of Shorelines, Proc. of the 9th Conf. on Coastal Eng., ASCE, 219-235.

Hwung, H.H. and Y.Y. Chen, 1981: The Development of the Velocity Distribution in Turbulent Plane Jet Interacting with Obliquely Wave, Proc. of the 5th Conf. on Ocean Eng. in Taiwan, 219-234 (in Chinese).

Jonsson, I.G., 1966: Wave Boundary Layers and Friction Factor, Proc. of the 10th Conf. on Coastal Eng., ASCE, 127-148.

Komar, P.D., 1973: Computer Models of Delta Growth Due to Sediment Input from Rivers and Longshore Transport, Soc. American Bull., Vol. 84, 2217-2226.

Longuet-Higgins, M. S., 1970: Longshore Currents Generated by Obliquely Incident Sea Waves, 1, 2, J. Geophys. Res., Vol. 75, No. 33, 6778-6789.

Tsuchiya, Y. and S. Yasuda, 1978: A Simple Model for Beach Evolution, Proc. the 25th Japanese Conf. on Coastal Eng., JSCE, 189-193 (in Japanese).

Willis, D. H., 1978a: An Alongshore Current Beach Evolution Model, Hydraulic Laboratory, Division of Mechanical Eng., National Res. Council of Canada, Rept. No. HY-92.

Willis, D. H., 1978b: Sediment Load Under Waves and Current, Proc. of the 16th Conf. on Coastal Eng., ASCE, 1627-1635.

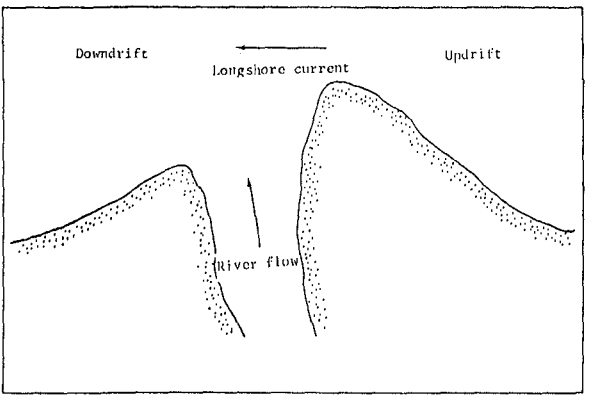

Fig. 1. Typical shoreline shape around a river mouth.

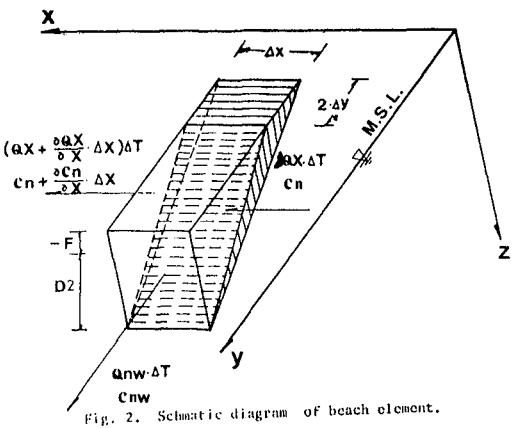

Fig. 2. Schmatic diagram of beach element.

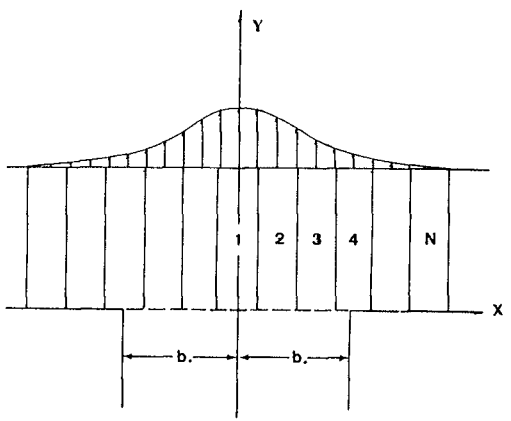

Fig. 3. Element layout around the river mouth.

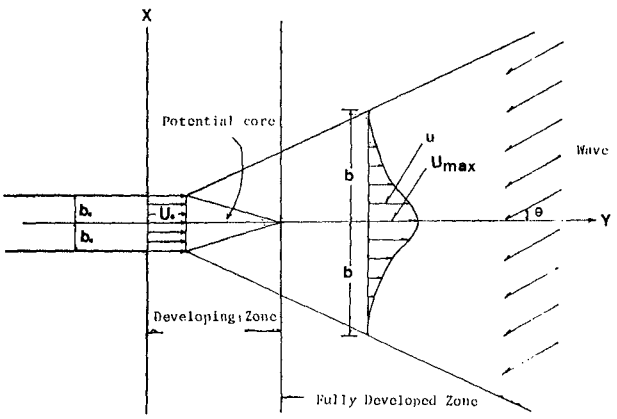

Fig. 4. Turbulent jet flow profile.

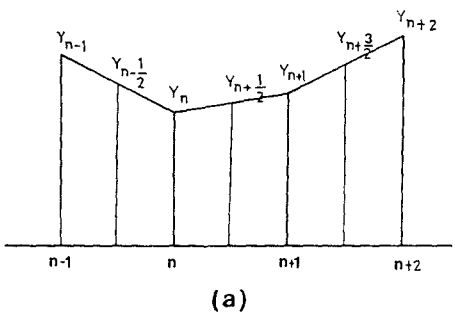

(a)

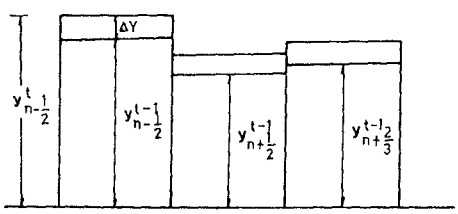

(b)

Fig. 5. Schematic diagram of grid element.

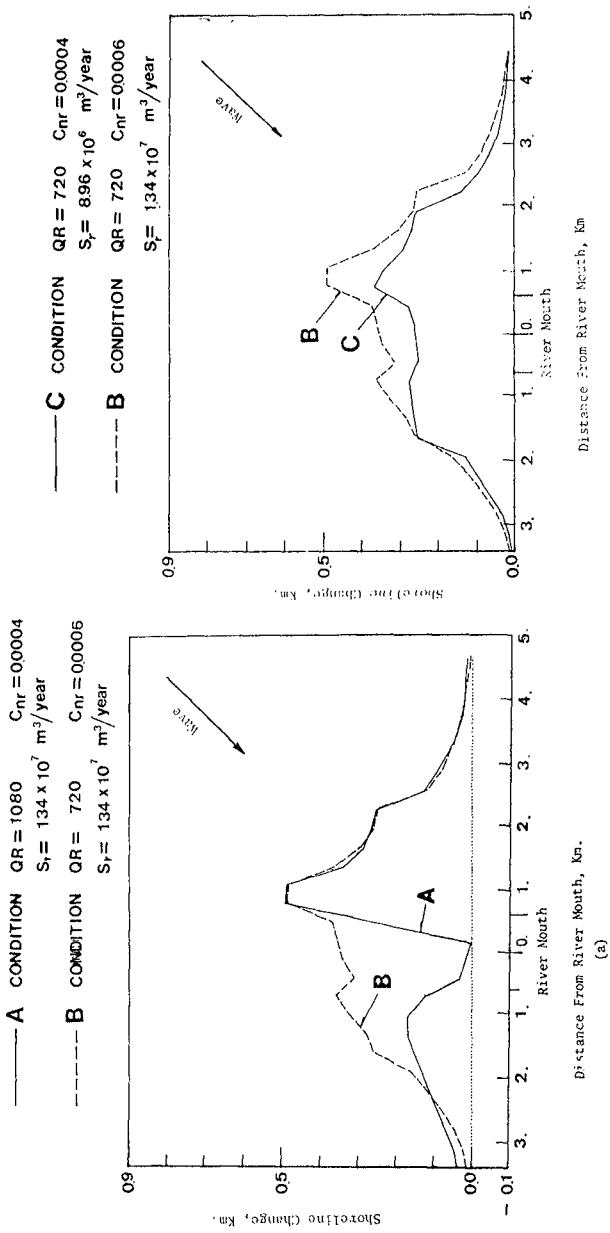

Fig. 6. Computed shoreline evolution around a river mouth. (Note that the scales used for horizontal and vertical coordinates are taken to be different).

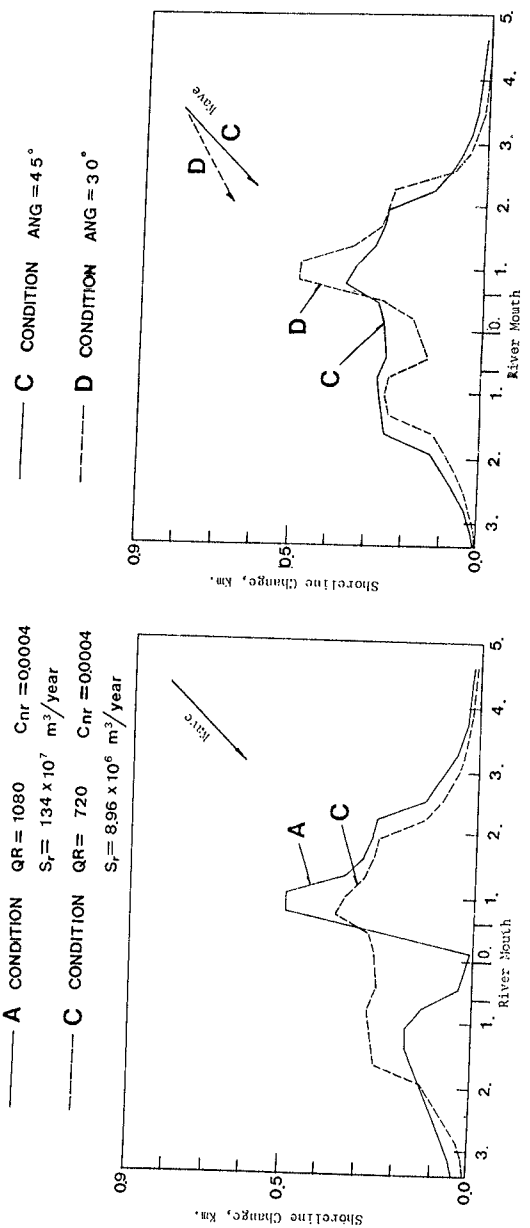

Fig. 6. Computed shoreline evolution around a river mouth. (Note that the scales used for horizontal and vertical coordinates are taken to be different).

Fig. 7. Actual shoreline changes around the Cho-Shui River mouth. (The shoreline is based on the minimum low tide).

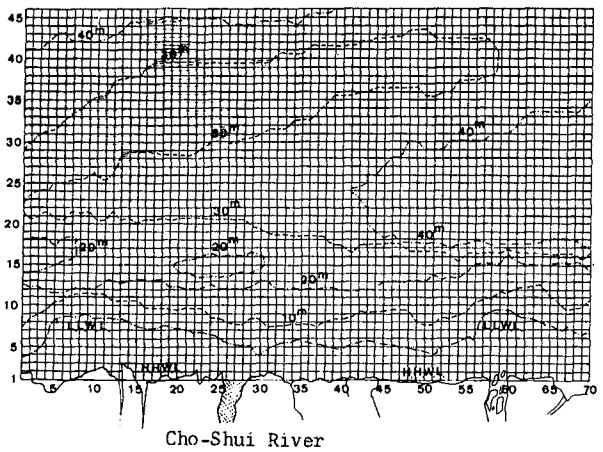

Fig. 8. Schmatic diagram at net-grid layout.

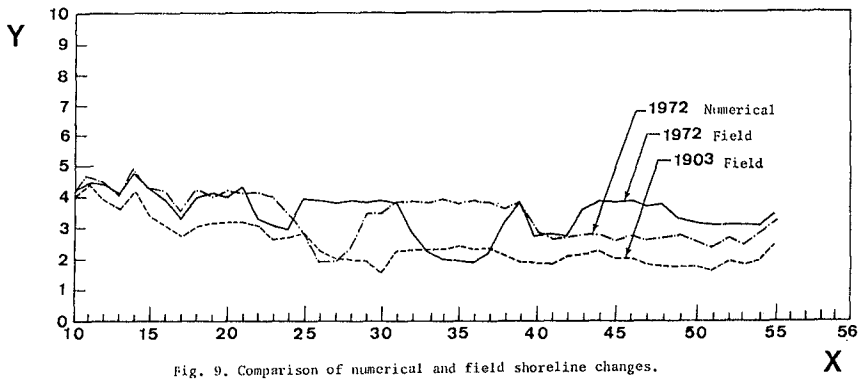

Fig. 9. Comparison of numerical and field shoreline changes.